UCLA
COMPUTATIONAL AND APPLIED MATHEMATICS

Mode-dependent Finite-difference Discretization of Linear Homogeneous Differential Equations

C.-C. Jay Kuo
Bernard C. Levy

September 1987

CAM Report 87-17

Department of Mathematics
University of California, Los Angeles
Los Angeles, CA. 90024-1555

September 25, 1987

Mode-dependent Finite-difference Discretization of Linear Homogeneous Differential Equations*

C.-C. Jay Kuo†

Bernard C. Levy††

Abstract

A new methodology utilizing the spectral analysis of local differential operators is proposed to design and analyze mode-dependent finite-difference schemes for linear homogeneous ordinary and partial differential equations. We interpret the finite-difference method as a procedure for approximating exactly a local differential operator over a finite-dimensional space of test functions called the coincident space and show that the coincident space is basically determined by the nullspace of the local differential operator. Since local operators are linear and approximately with constant coefficients, we introduce a transform domain approach to perform the spectral analysis. For the case of boundary-value ODEs, a mode-dependent finite-difference scheme can be systematically obtained. For boundary-value PDEs, mode-dependent 5-point, rotated 5-point and 9-point stencil discretizations for the Laplace, Helmholtz and convection-diffusion equations are developed. The effectiveness of the resulting schemes is shown analytically, as well as by considering several numerical examples.

Key Words: convection-diffusion equation, finite-difference method, Helmholtz equation, high order schemes, Laplace equation, mode-dependent discretization, spectral analysis, transform domain.

---

* This work was supported in part by the Army Research Office under No. DAAL03-86-K-0171, in part by the Advanced Research Projects Agency monitored by ONR under contract N00014-81-K-0742, and in part by the Department of Energy under contract DE-FG03-87ER25037.

† Department of Mathematics, University of California, Los Angeles, CA 90024.

† Department of Electrical and Computer Engineering, University of California, Davis, CA 95616.

1. Introduction

In order to derive a finite-difference approximation for the derivative of a smooth function, a common procedure is to use a Taylor series to expand the function locally and to select the coefficients such that the order of the discretization error is as high as possible. This procedure is based on the assumption that smooth functions can be well approximated by polynomials locally, and in fact it can be shown that the resulting finite-difference approximation is exact for low order polynomials. However, when the function is exponentially increasing (decreasing) or highly oscillatory, the polynomial representation becomes poor and better finite-difference schemes can be derived by requiring that the derivative of exponential or trigonometric functions should be approximated exactly. In this paper, polynomials, exponential and trigonometric functions are all viewed as modes, and finite-difference schemes obtained by an exact approximation of the derivative of a certain number of modes are called *mode-dependent finite-difference* schemes. These modes are the *coincident modes* and the space spanned by them is the *coincident space*.

Historically, the idea of selecting exponential functions as coincident modes was first suggested by Allen and Southwell [1] for discretizing the convection-diffusion equation. An important feature of this problem is that there are large first-order terms in the governing second-order PDE. Due to these large first-order terms, there exists a boundary layer which cannot be well approximated by polynomials. The use of trigonometric functions as coincident modes was first discussed by Gautschi [19] for the numerical integration of ODEs which have periodic or oscillatory solutions whose periods can be estimated in advance. In addition, high order finite-difference schemes for the Laplace equation were derived by choosing some particular polynomials as coincident modes [32].

Although the concept of a mode-dependent finite-difference discretization procedure has been known for years and mentioned repeatedly in the literature (see for examples the references appearing in Section 6), few theoretical results about this method have been obtained until now. Important problems, such as whether the mode-dependent finite-difference discretization procedure can always be efficiently applied and how to design such a scheme, remain open. This paper provides

a methodology utilizing the spectral analysis of local differential operators to answer these questions. To avoid unnecessary distractions, we will concentrate on 1D and 2D homogeneous boundary-value problems. However, the general methodology described here also applies to initial value problems as well as nonhomogeneous equations. We will demonstrate this point by referring to some related work.

Since a differential operator is well approximated locally by a linear constant-coefficient operator, the spectral analysis of this local operator becomes relatively easy and a transform domain analysis can be conveniently applied. In the transform domain, the differential and difference operators are algebraic expressions in terms of the complex frequencies s and z. We interpret the mode-dependent finite-difference discretization procedure as a way to specify how these two expressions match each other at a certain number of frequencies in the transform domain. This transform domain viewpoint helps us to gain a better understanding of existing mode-dependent finite-difference schemes and serves as a basis for designing new schemes.

We apply the same methodology to both ODEs and PDEs, and develop several mode-dependent finite-difference schemes. The main results include an $(R+1)$-point mode-dependent central difference scheme for an R th-order boundary-value ODE, and 5-point, rotated 5-point, 9-point stencil discretizations for the 2D Laplace, Helmholtz and convection-diffusion equations. The mode-dependent finite-difference schemes for the Laplace equation are the same as the conventional ones. However, we present a new derivation. The mode-dependent 5-point and 9-point stencil discretizations of the Helmholtz and convection-diffusion equations are new and have an accuracy proportional to $O(h^2)$ and $O(h^6)$ respectively.

This paper is organized as follows. In Section 2, we describe the mode-dependent finite-difference approximation concept in both the space and transform domains. In Section 3, we study the discretization of boundary-value ODEs. The problem of determining the coincident space for homogeneous ODEs is discussed and a mode-dependent finite-difference scheme is presented. This scheme is shown to be exact for constant-coefficient ODEs and has a high degree of accuracy for

ODEs with smoothly varying coefficients. The extension to the problem of discretizing nonhomogeneous ODEs is briefly addressed. In Section 4, we generalize the methodology from one to two dimensions. In particular, we use the Laplace, Helmholtz and convection-diffusion equations as examples to demonstrate the mode-dependent finite-difference discretization procedure for PDEs. Numerical examples are presented in Section 5. Section 6 discusses several previous related contributions. The main purpose of this section is to organize the literature concerning the mode-dependent finite-difference approximation so that more examples will be accessible to interested readers. Some generalizations and concluding remarks are given in Section 7.

2. Mode-dependent finite-difference discretization

Consider the class of functions of the form

$$u(x) = \sum_{k=1}^{K} [\, c_{k0} + c_{k1}x + c_{k2}\frac{x^2}{2!} + \cdots + c_{kn_k}\frac{x^{n_k}}{(n_k)!} \,] \, e^{s_k x} \ ,$$

where each term $x^p e^{s_k x}$, $0 \le p \le n_k$, is called a *mode* of order p at the *frequency* s_k. We are interested in approximating a linear R th-order constant-coefficient differential operator operating on $u(x)$,

$$L(D) = \sum_{r=0}^{R} a_r D^r \ ,$$

where $D = \frac{d}{dx}$, by a $(r_2 - r_1 + 1)$-point finite-difference operator

$$L_d(E) = \sum_{r=r_1}^{r_2} b_r E^r \ ,$$

where E is the shift operator defined on a uniform grid G_h with spacing h, i.e. for nh, $(n+r)h \in G_h$, $E^r u(nh) = u((n+r)h)$. L_d corresponds to a forward, backward or central difference operator depending on whether $r_1 = 0$, $r_2 = 0$ or $-r_1 = r_2$, respectively. We use

$$P_n(s) = \{\, u(x) : \quad u(x) = e^{sx} \sum_{k=0}^{n} c_k \, x^k \quad \} \tag{2.1}$$

to represent the space spanned by polynomials of degree at most n multiplied by the factor e^{sx}. A mode-dependent finite-difference discretization scheme is obtained by selecting the coefficients b_r of L_d such that

$$[\, L_d(E) - L(D) \,] \, u(x) = 0 \qquad \text{for} \quad u(x) \in C \quad \text{and} \quad x \in G_h \ , \tag{2.2}$$

where C, called the coincident space of the operator L_d, is the direct sum of subspaces of the form (2.1), i.e.

$$C = \bigoplus_{k=1}^{K} P_{n_k}(s_k) \ . \tag{2.3}$$

A mode in the coincident space C is called a coincident mode, and its frequency is called a coincident frequency.

The mode-dependent finite-difference scheme can be conveniently formulated in the transform domain. $L(s)$ is obtained by replacing D with s through the use of the Laplace transform in the s-domain,

$$L(s) = \sum_{r=0}^{R} a_r s^r \ ,$$

while $L_d(z)$ is obtained by replacing E with z through the use of the Z-transform in the z-domain,

$$L_d(z) = \sum_{r=r_1}^{r_2} b_r z^r = \sum_{r=r_1}^{r_2} b_r e^{rsh} \ .$$

where the last equality is due to the fact that since E is related to D via $E = e^{hD}$ [11], we have $z = e^{sh}$. Then, we can express the difference Δ between L and L_d in terms of a single variable s in the transform domain

$$\Delta(s) = L_d(e^{sh}) - L(s) \ ,$$

and the characterization (2.2)-(2.3) of the mode-dependent finite-difference scheme can be equivalently stated in the transform domain as

$$\Delta^{(p)}(s_k) = 0 \ , \quad 0 \le p \le n_k \ , \ 1 \le k \le K \ , \tag{2.4}$$

where $\Delta^{(n)}(s_k) = \dfrac{d^n \Delta(s)}{ds^n}\Big|_{s=s_k}$. Let $Q(x)$ be an arbitrary polynomial. Then, the characterization (2.4) is in fact a direct consequence of the equalities

$$L(\frac{\partial}{\partial x})[Q(x)e^{sx}] = L(\frac{\partial}{\partial x})[Q(\frac{\partial}{\partial s})e^{sx}] = Q(\frac{\partial}{\partial s})[L(\frac{\partial}{\partial x})e^{sx}] = Q(\frac{\partial}{\partial s})[L(s)e^{sx}] \ ,$$

and

$$L_d(E)[Q(x)e^{sx}] = L_d(E)[Q(\frac{\partial}{\partial s})e^{sx}] = Q(\frac{\partial}{\partial s})[L_d(E)e^{sx}] = Q(\frac{\partial}{\partial s})[L_d(e^{sh})e^{sx}] \ .$$

It is usually easier to determine the coefficients b_r of the mode-dependent finite-difference discretization scheme by applying (2.4) rather than (2.2) and (2.3).

Example 1: To illustrate the mode-dependent discretization procedure described above, the coincident modes and coefficients of several 3-point central difference schemes for the first-order derivative D are listed in Table 1.

modes	$1,\ e^{\sigma x}\sin(\omega x),\ e^{\sigma x}\cos(\omega x)$	$1,\ e^{\sigma x},\ xe^{\sigma x}\ (\ \sigma \neq 0\ )$
b_{-1}	$\dfrac{e^{\sigma h}[\sigma\sin(\omega h)-\omega\cos(\omega h)]+\omega}{2\sin(\omega h)[\cos(\omega h)-\cosh(\sigma h)]}$	$\dfrac{(1-\sigma h)e^{\sigma h}-1}{2h\,[\cosh(\sigma h)-1]}$
b_0	$\dfrac{\omega\cos(\omega h)\sinh(\sigma h)-\sigma\sin(\omega h)\cosh(\sigma h)}{\sin(\omega h)[\cos(\omega h)-\cosh(\sigma h)]}$	$\dfrac{\sigma h\cosh(\sigma h)-\sinh(\sigma h)}{h\,[\cosh(\sigma h)-1]}$
b_1	$\dfrac{e^{-\sigma h}[\sigma\sin(\omega h)+\omega\cos(\omega h)]-\omega}{2\sin(\omega h)[\cos(\omega h)-\cosh(\sigma h)]}$	$\dfrac{-(1+\sigma h)e^{-\sigma h}+1}{2h\,[\cosh(\sigma h)-1]}$
modes	$1,\ e^{\sigma_1 x},\ e^{\sigma_2 x}\ (\ \sigma_1 \neq \sigma_2\ )$	$1,\ x,\ x^2$
b_{-1}	$\dfrac{1}{2}\dfrac{\sigma_2(1-e^{\sigma_1 h})-\sigma_1(1-e^{\sigma_2 h})}{\sinh[(\sigma_2-\sigma_1)h\,]+\sinh(\sigma_1 h)-\sinh(\sigma_2 h)}$	$\dfrac{-1}{2h}$
b_0	$\dfrac{\sigma_2\sinh(\sigma_1 h)-\sigma_1\sinh(\sigma_2 h)}{\sinh[(\sigma_2-\sigma_1)h\,]+\sinh(\sigma_1 h)-\sinh(\sigma_2 h)}$	0
b_1	$\dfrac{1}{2}\dfrac{\sigma_1(1-e^{-\sigma_2 h})-\sigma_2(1-e^{-\sigma_1 h})}{\sinh[(\sigma_2-\sigma_1)h\,]+\sinh(\sigma_1 h)-\sinh(\sigma_2 h)}$	$\dfrac{1}{2h}$

Table 1: The approximation of the first-order derivative D ($L(s) = s$) by a central mode-dependent finite-difference scheme.

3. Discretization of boundary-value ODEs

3.1 Homogeneous ODEs

Consider an R th-order homogeneous two-point boundary value problem on [0,1]. For convenience, we consider the case $R=2m$. The case $R=2m+1$ gives rise to a similar analysis. The equation is written as

$$L\ u = 0\ , \qquad \text{where}\ \ L = \sum_{r=0}^{2m} a_r(x) D^r \ \ \text{and}\ \ a_{2m}(x) = 1\ , \tag{3.1}$$

with given boundary conditions. We discretize (3.1) on a uniform grid with spacing h by a $(2m+1)$-point central difference scheme,

$$L_d\ U = 0\ , \qquad \text{where} \qquad L_d = \sum_{r=-m}^{m} b_r(nh) E^r\ , \tag{3.2}$$

and U is the estimate of u on grid points. Suppose that ϕ is an arbitrary function in the nullspace N_L of operator L, and that N_L is contained in the coincident space C of L_d. Then, since

$$L\ \phi = 0 \qquad \text{and} \qquad [\ L_d - L\ ]\ \phi = 0\ ,$$

we obtain

$$L_d\ \phi = 0\ . \tag{3.3}$$

Since the discretization for an arbitrary function in the nullspace N_L is exact, we conclude that equation (3.1) is exactly discretized by (3.2).

The nullspace N_L is easy to find if the coefficients $a_r(x)$ of L are constant. Even if these coefficients are not constant but smoothly-varying, L still can be well approximated by a constant-coefficient operator in a local region. This simplification is always assumed for finite-difference schemes since the finite-difference method is a local approximation method. For convenience, we drop the spatial dependency of coefficients $a_r(x)$ and $b_r(x)$, and use the notation $a_r \approx a_r(x_0)$ and $b_r \approx b_r(x_0)$ inside operators L and L_d for the rest of this paper. If $a_r(x)$ and $b_r(x)$ are spatially varying, the discussion is understood to be a *local* analysis in the neighborhood of x_0.

The spectral analysis of a linear constant-coefficient operator $L = \sum_{r=0}^{2m} a_r D^r$ can be easily

performed in the transform domain. We choose the coincident frequencies to be roots of the characteristic equation,

$$L(s) = s^{2m} + a_{2m-1}s^{2m-1} + \cdots + a_1 s + a_0 = 0 .$$

In general, $L(s)$ can be factored as

$$L(s) = \prod_{k=1}^{K} (s - s_k)^{n_k} , \qquad \text{where} \quad \sum_{k=1}^{K} n_k = 2m ,$$

and s_k is known as a *natural frequency* of L of order n_k. As a consequence, the operator L has the $2m$-dimensional nullspace

$$N_L = \bigoplus_{k=1}^{K} P_{n_k-1}(s_k) .$$

A $(2m+1)$-point finite difference scheme can be uniquely determined by a $(2m+1)$-dimensional coincident space C. However, since a homogeneous finite-difference equation such as (3.2) can be scaled arbitrarily, a $2m$-dimensional coincident space C is sufficient to specify L_d in (3.2). So, letting

$$C = N_L ,$$

we have an exact discretization scheme for (3.1). For this choice, L_d can be determined easily as

$$L_d(z) = A\ z^{-m} \prod_{k=1}^{K} (z - z_k)^{n_k} , \qquad \text{where} \quad z_k = e^{s_k h} , \tag{3.4}$$

where A is a scaling factor and the multiplication factor z^{-m} is due to the fact that we want $L_d(z)$ to be a central difference scheme. This can be verified by substituting $L(s)$ and $L_d(e^{sh})$ back into (2.4).

Hence, after inverse transformation, we obtain the following mode-dependent finite-difference scheme for (3.1) in the space domain

$$L_d U = 0 , \quad \text{where} \quad L_d(E) = A\ E^{-m} \prod_{k=1}^{K} (E - e^{s_k h})^{n_k} , \tag{3.5}$$

and s_k is a natural frequency of L of order n_k. The scaling factor A does not affect the solution of the system of equations (3.5). However, in order to analyze the discretization error $\Delta(s)$ appropriately, it is important to choose A such that $L_d(e^{sh})$ and $L(s)$ are consistent over fine

grids. This consideration requires that the scaling factor A of (3.5) should be proportional to $\frac{1}{h^{2m}}$, as h goes to zero.

Example 2: (1D Laplace equation) For $L(D) = D^2$, we know that $N_L = \{ 1 , x \}$. The coincident modes have the same frequency $s_k = 0$. According to (3.5), we have

$$L_d(E) = A\ E^{-1}\ (E - 1)^2 = A\ (E - 2 + E^{-1}) . \tag{3.6}$$

If we choose $C = N_L + \{ x^2 \}$, the constant A can be uniquely determined. Solving $Lx^2 = L_d x^2$, where $x \in G_h$, we find that $A = \frac{1}{h^2}$. Then, (3.6) reduces to the standard 3-point central difference scheme.

Example 3: (1D convection-diffusion equation) The differential operator is $L(D) = D^2 - a_1 D$, where $a_1 \neq 0$. In this case, $N_L = \{ 1 , e^{a_1 x} \}$ and $s_k = 0 , a_1$. Therefore, by (3.5), we have

$$L_d(E) = A\ E^{-1}\ (E - 1)\ (E - e^{a_1 h}) = A\ [\ E - (1+e^{a_1 h}) + e^{a_1 h} E^{-1}\ ] . \tag{3.7}$$

In particular, if $C = N_L + \{ x \}$, we find that $A = \frac{a_1}{h(e^{a_1 h}-1)}$. Then, (3.7) is identical to the scheme considered by Allen and Southwell [1].

For comparison, consider the conventional finite-difference scheme for (3.1),

$$L_{d,c} U = 0 , \quad \text{where} \quad L_{d,c}(E) = \sum_{r=0}^{2m} a_r h^{-r} D^r_{d,2m+1}(E) , \tag{3.8}$$

where $h^{-r} D^r_{d,2m+1}(E)$ denotes the $(2m+1)$-point central difference operator for the rth-order derivative D^r which is obtained by selecting $C = P_{2m}(0)$ as coincident space, and by requiring consistency over fine grids. Then, by comparing (3.5) and (3.8), we see that the mode-dependent scheme (3.5) is obtained by discretizing term by term the product form of the differential operator $L(D)$, whereas the conventional scheme (3.8) is found by discretizing term by term the summation form of $L(D)$.

According to the above discussion, the approximation of the differential operator $L(D)$ in (3.1) by $L_d(E)$ given by (3.5) does not give rise to any discretization error when the coefficients

a_r are constant. This fact is also supported by numerical results.

Of course, the mode-dependent scheme (3.5) gives rise to a discretization error when the coefficients a_r are spatially varying. This discretization error depends on the smoothness of the ODE coefficients and the grid size h. However, the exact form of this dependency is still unknown, and we have yet to develop a general procedure for estimating the size of the error in this case. In Section 5, we use a 1D convection-diffusion equation as a test problem and find that the error of the mode-dependent scheme is proportional to $O(\varepsilon h^2)$ while that of the conventional scheme is proportional to $O(h^2)$, where ε is the first order derivative of the coefficient function. The mode-dependent scheme is always better than the conventional central-difference scheme in this test problem and the improvement in accuracy offered by the mode-dependent scheme becomes larger as the coefficient of the convection-diffusion equation becomes smoother.

3.2 Extensions to nonhomogeneous ODEs

Suppose that (3.1) includes a driving function $f(x)$, so that

$$L\ u - f = 0\ . \tag{3.9}$$

By performing a Taylor series expansion of $f(x)$ in the vicinity of a discretization point x_0, we can assume that f is approximated locally by a polynomial of low degree, i.e.

$$f(x) \approx c_0 + c_1\, x + c_2\, x^2 + \cdots\ .$$

A general discretization scheme for (3.9), which has been proposed in the context of the OCI and HODIE methods [4][7][31], is

$$L_d\ U - I_d\ f = L_d\ U - I_d\ Lu = 0\ , \tag{3.10}$$

where I_d is an averaging operator.

The set of functions whose images through L are polynomials of degree less or equal to l defines the space

$$P_{L,l} = \{\ u(x) : Lu = \sum_{r=0}^{l} p_r x^r\ \}\ .$$

Note that since the coefficients p_r above can all be selected equal to zero, N_L is also included in

$P_{L,l}$. The space $P_{L,l}$ will be used here to approximate the solution space of equation (3.9). Suppose that ψ is an arbitrary function of the space $P_{L,l}$. Ideally, we want

$$L_d\ \psi - I_d\ L\ \psi = 0\ , \tag{3.11}$$

in order to guarantee that the discretization (3.10) of the nonhomogeneous equation (3.9) is exact in the approximated solution space $P_{L,l}$.

In particular, if I_d is chosen to be the identity operator I, (3.11) becomes

$$(\ L_d - L\ )\ \psi = 0\ . \tag{3.12}$$

Therefore, the coincident space C of the finite-difference operator L_d for the nonhomogeneous equation (3.9) has to be

$$C = P_{L,l}\ .$$

The major disadvantage of this choice is that the dimension of C is larger than that of N_L. Hence, a finite-difference method with more than $(2m+1)$-points will be necessary and more computations will be required.

The purpose of introducing I_d is to reduce the dimension of the coincident space. For a $(2m+1)$-point finite-difference scheme, we can decompose the discretization scheme (3.10) into two steps. First, by choosing $C = P_{L,0}$, we can uniquely determine L_d. Then, by using an arbitrary function ψ of the space $P_{L,l} \ominus P_{L,0}$ as a test function for (3.11), we can solve for the coefficients of I_d. This procedure is illustrated by the following example.

Example 4: (1D Poisson equation) In this case, we have $L(D) = D^2$, $N_L = \{\ 1, x\ \}$, and $P_{L,l} = \{\ 1, x, x^2, x^3, \cdots, x^{l+2}\ \}$. By choosing $C = P_{L,0}$, we know from example 2 that

$$L_d(E) = \frac{1}{h^2}\ (\ E - 2 + E^{-1}\ )\ .$$

Assuming that $I_d(E) = d_{-1}E^{-1} + d_0 + d_1\ E$ with respect to the same grid G_h and solving (3.11) with L_d given above and $\psi = x^3, x^4$, we obtain

$$I_d(E) = \frac{1}{12}E^{-1} + \frac{5}{6} + \frac{1}{12}E\ .$$

Then, for this case, the discretization (3.10) corresponds to the classical Stormer-Numerov

approximation, and it is exact for any function in the space $P_{L,2}$. More generally, we call $P_{L,l}$ the *generalized coincident space* $C_g(\,L_d\,,\,I_d\,)$ for the approximation (3.10) of (3.9). Note that the dimension of C_g for the above example is 5, and that there are 5 independent parameters in $(\,L_d\,,\,I_d\,)$ since (3.11) can be scaled by an arbitrary constant.

The above approach is different from the HODIE method. For an R th-order nonhomogeneous ODE, the HODIE method uses polynomials of degree less or equal to n, i.e. $P_n(0)$ with $n > R$, as the generalized coincident space C_g for equation (3.10). It does not exploit any special structure of the differential operator L. In contrast, our mode-dependent method uses the approximated solution space $P_{L,n-R}$ as the generalized coincident space C_g. Hence, a spectral analysis of the operator L is necessary. In particular, when $L = D^R$, $P_{L,n-R}$ is the same as $P_n(0)$. Then, there is no difference between the HODIE and mode-dependent methods.

The determination of the averaging operator I_d for the HODIE method has been discussed in detail [7][31]. For example, the operator I_d may be defined on an *auxiliary* grid different from the discretization grid G_h. A similar approach can also be used to design I_d for the mode-dependent method. Note that the selection of the averaging operator I_d has no effect on functions in the nullspace N_L. Therefore, the coincident space C of L_d has to contain N_L so that the discretization error for functions in N_L can be eliminated by choosing an appropriate L_d.

In this paper, we focus primarily on the determination of the coincident space C and of the finite-difference operator L_d. In the next section, we will therefore restrict our attention to *homogeneous* boundary-value PDEs and we will attempt to extend the methodology developed in this section to the discretization of this specific class of PDE problems.

4. Discretization of boundary-value PDEs

Consider a general two-dimensional boundary-value PDE on the square $[0,1]^2$

$$L(D_x,D_y)\,u = 0\,, \quad \text{where} \quad L(D_x,D_y) = \sum_{r,s} a_{r,s} D_x^r D_y^s\,, \tag{4.1}$$

with $D_x^r = \dfrac{\partial^r}{\partial x^r}$ and $D_y^s = \dfrac{\partial^s}{\partial y^s}$, and with appropriate boundary conditions. We discretize (4.1) with the finite-difference scheme

$$L_d(E_x,E_y)\,U = 0\,, \quad \text{where} \quad L(E_x,E_y) = \sum_{r,s} b_{r,s} E_x^r E_y^s\,, \tag{4.2}$$

and where E_x and E_y are respectively the shift operators in the x- and y-directions on the grid G_{h_x,h_y}. Relying on a natural generalization of the 1D case, we have the following associations between the 2D space domain operators and transform domain variables

$$D_x \longleftrightarrow s_x\,, \quad D_y \longleftrightarrow s_y\,, \quad E_x \longleftrightarrow z_x\,, \quad E_y \longleftrightarrow z_y\,.$$

where $s_x = \sigma_x + i\,\omega_x$ and $s_y = \sigma_y + i\,\omega_y$. They are related via $E_x = e^{h_x D_x}$, $E_y = e^{h_y D_y}$, $z_x = e^{h_x s_x}$ and $z_y = e^{h_y s_y}$. To simplify the following discussion, we will only consider the case $h_x = h_y = h$.

Substituting $e^{s_x x + s_y y}$ inside (4.1), we obtain the characteristic equation

$$\sum_{r,s} a_{r,s} s_x^r s_y^s = 0\,. \tag{4.3}$$

There are two complex variables in (4.3), but since we have only one (complex) equation, there are infinitely many solutions to this equation and therefore infinitely many modes in N_L. It is not possible to approximate all modes in N_L exactly. Thus, we have to select a finite-dimensional subspace $D_L \subset N_L$, called the dominant-mode space, as the coincident space C for L_d. The determination of D_L depends on a rough estimation of the local behavior of the solution. This information is usually provided by the structure of the PDE operator and the corresponding boundary conditions. In this section, we restrict our attention to the case where the dominant modes are either oscillating or exponentially growing (decaying). In other words, coincident frequencies are selected among the sets

$$\{\ (s_x,s_y) : (s_x,s_y) = (\sigma_x,\sigma_y)\ \} \quad or \quad \{\ (s_x,s_y) : (s_x,s_y) = (i\,\omega_x, i\,\omega_y)\ \}\ . \tag{4.4}$$

We do not consider complex coincident frequencies, since they generally lead to discretization schemes with complex coefficients which complicate the solution procedure. However, even under (4.4), the mode-dependent concept still does not lead to a unique discretization scheme. By taking into account the symmetrical property of the spectra of the differential and difference operators and the solubility of the resulting finite-difference schemes, we can further constrain ourselves within a much smaller design space. In the following, the 5-point, rotated 5-point and 9-point stencil discretizations for the Laplace, Helmholtz and convection-diffusion equations will be used as examples to demonstrate the mode-dependent discretization concept.

4.1 Laplace equation

For the Laplace equation, we have $L(D_x,D_y) = D_x^2 + D_y^2$. Since only one frequency $(s_x,s_y) = (0,0)$ satisfies the characteristic equation and belongs to the sets (4.4) of interest, (0,0) is selected as the unique coincident frequency. In this case, the mode-dependent scheme is the same as the conventional scheme.

The following 5-point, rotated 5-point and 9-point stencil discretization schemes have been derived by several approaches [11][25][32],

$$L_{d,+}(E_x,E_y) = \frac{1}{h^2}\ (\ E_x + E_x^{-1} + E_y + E_y^{-1} - 4\ )\ , \tag{4.5}$$

$$L_{d,\times}(E_x,E_y) = \frac{1}{2h^2}\ (\ E_xE_y + E_x^{-1}E_y + E_xE_y^{-1} + E_x^{-1}E_y^{-1} - 4\ )\ , \tag{4.6}$$

$$L_{d,9} = \frac{1}{6h^2}\ [\ 4(E_x+E_x^{-1}+E_y+E_y^{-1}) + (E_xE_y+E_x^{-1}E_y+E_xE_y^{-1}+E_x^{-1}E_y^{-1}) - 20\ ]\ . \tag{4.7}$$

It is well known that they have respectively an accuracy of $O(h^2)$, $O(h^2)$ and $O(h^6)$ when used to discretize the Laplace equation [25].

Here, we present another derivation of these schemes by matching $L(s_x,s_y)$ and $L_d(z_x,z_y)$ at the coincident frequency (0,0) in the transform domain. As before, we consider the expansion of $\Delta = L_d - L$ around (0,0),

$$\Delta(s_x,s_y) = \Delta^{(0,0)}(0,0) + \Delta^{(1,0)}(0,0)s_x + \Delta^{(0,1)}(0,0)s_y + \frac{1}{2}\,[\,\Delta^{(2,0)}(0,0)s_x^2$$

$$+ \Delta^{(1,1)}(0,0)2s_x s_y + \Delta^{(0,2)}(0,0)s_y^2\,] + \sum_{\substack{p+q\geq 3\\ p,q\geq 0}} \Delta^{(p,q)}(0,0)\frac{1}{p!q!}s_x^p s_y^q\,, \qquad (4.8)$$

where

$$\Delta^{(p,q)}(0,0) = \frac{\partial^{p+q}\Delta(s_x,s_y)}{\partial^p s_x \partial^q s_y}\Big|_{(s_x,s_y)=(0,0)}\,,$$

which is a function of the grid size h. Hence, (4.8) is in fact a power series of h. Our derivation attempts to make the order of the residual terms in (4.8) as high as possible.

The discretization schemes (4.5) and (4.6) can be derived by requiring respectively that

$$\Delta^{(0,0)}(0,0) = \Delta^{(1,0)}(0,0) = \Delta^{(0,1)}(0,0) = \Delta^{(2,0)}(0,0) = \Delta^{(0,2)}(0,0) = 0\,,$$

and

$$\Delta^{(0,0)}(0,0) = \Delta^{(1,0)}(0,0) = \Delta^{(0,1)}(0,0) = \Delta^{(1,1)}(0,0) = \Delta^{(2,0)}(0,0) = \Delta^{(0,2)}(0,0) = 0\,.$$

Note the similarity between the the above requirements and (2.4). The above choice of constraint $\Delta^{(p,q)}(0,0) = 0$ has taken into account the specific structure of operators $L_{d,+}$, $L_{d,\times}$ and L. For example, in the case of $L_{d,\times}$, the symmetry properties of $L_{d,\times}$ imply that $\Delta^{(2,0)}(0,0) = \Delta^{(0,2)}(0,0)$, so that among the six constraints which are used to specify $L_{d,\times}(E_x,E_y)$, only five are independent.

By setting the coefficients of low order terms in (4.8) equal to zero, it is possible to obtain various high-order finite-difference discretization schemes. For example, to obtain the 9-point scheme (4.7), we need only to impose the requirement that this scheme should have an accuracy of $O(h^6)$ for modes satisfying the characteristic equation $s_x^2 + s_y^2 = 0$. Then, substituting the identity $s_x^2 + s_y^2 = 0$ inside (4.8) and setting coefficients up to order h^5 equal to zero, we obtain nine independent constraints which specify (4.7) uniquely.

4.2 Helmholtz equation

For the Helmholtz equation, we have

$$L(D_x,D_y) = D_x^2 + D_y^2 + \lambda^2\,.$$

If s_x and s_y are purely imaginary, the characteristic equation becomes

$$\omega_x^2 + \omega_y^2 = \lambda^2 , \tag{4.9}$$

which is a circle in the ω_x-ω_y plane, centered at the origin and with radius $|\lambda|$. There are infinitely many natural frequencies and, hence, there are many different ways to select coincident frequencies. In this section, we design mode-dependent 5-point, rotated 5-point and 9-point stencil discretization schemes based on the following two considerations. First, if there is no further information about the dominant modes, a reasonable strategy is to distribute coincident frequencies uniformly along the contour (4.9). Second, we want to preserve the symmetry properties of L so that the resulting discretization scheme is in a simple form and can easily be implemented.

Let us select

$$(\omega_x , \omega_y) = (|\lambda| \cos(\frac{n}{2}\pi + \frac{1}{4}\pi) , |\lambda| \sin(\frac{n}{2}\pi + \frac{1}{4}\pi)) , \qquad 0 \le n \le 3 ,$$

as coincident frequencies as shown in Figure 1(a). With this choice, the discretization along the x- and y-directions can be treated independently. The resulting scheme is

$$L_d(E_x, E_y) = A \ [\ E_x^{-1} - 2\cos(\frac{|\lambda|}{\sqrt{2}}h) + E_x + \kappa(E_y^{-1} - 2\cos(\frac{|\lambda|}{\sqrt{2}}h) + E_y \ ) \ ] .$$

Two parameters A and κ remain undetermined in the above expression. The parameter κ is selected such that the discretization error $\Delta(s_x, s_y)$ at natural frequencies is proportional to $O(h^2)$, and the parameter A is used to normalize the above scheme so that L_d is consistent with L. A simple choice of κ and A for the Helmholtz equation is $\kappa = 1$ and $A = \frac{1}{h^2}$. Hence, this gives a symmetrical 5-point stencil discretization operator

$$L_{d,+}(E_x, E_y) = \frac{1}{h^2} \ [\ E_x^{-1} + E_x + E_y^{-1} + E_y - 4\cos(\frac{|\lambda|}{\sqrt{2}}h) \ ] . \tag{4.10}$$

Rotating the above four coincident frequencies in the transform domain and the above 5-point stencil in the space domain by an angle $\frac{1}{4}\pi$, we obtain another mode-dependent 5-point stencil discretization. In this scheme, the coincident frequencies become

$$(\omega_x , \omega_y) = (|\lambda| \cos(\frac{n}{2}\pi) , |\lambda| \sin(\frac{n}{2}\pi)) , \qquad 0 \le n \le 3 .$$

as shown in Figure 1(b), and the resulting 5-point stencil operator is

$$L_{d,\times}(E_x,E_y) = \frac{1}{2h^2}\,[\,E_x^{-1}E_y^{-1} + E_x^{-1}E_y + E_xE_y^{-1} + E_xE_y - 4\cos(|\lambda|h)\,]\,. \qquad (4.11)$$

Notice that this rotated 5-point stencil can be viewed as corresponding to a discretization scheme on a grid with spacing $\sqrt{2}h$. By appropriately combining (4.10), (4.11) and adding a constant term, we obtain the 9-point stencil discretization operator,

$$L_{d,9}(E_x,E_y) = \frac{\gamma_\times}{\gamma_\times+\gamma_+}L_{d,+}(E_x,E_y) + \frac{\gamma_+}{\gamma_\times+\gamma_+}L_{d,\times}(E_x,E_y) - \frac{\gamma_\times\,\gamma_+}{\gamma_\times+\gamma_+}\,. \qquad (4.12)$$

Then, if

$$\gamma_\times = L_{d,\times}(e^{i\frac{|\lambda|}{\sqrt{2}}h},e^{i\frac{|\lambda|}{\sqrt{2}}h}) = \frac{1}{h^2}\,[\,\cos(\sqrt{2}|\lambda|h) + 1 - 2\cos(|\lambda|h)\,]\,,$$

$$\gamma_+ = L_{d,+}(e^{i|\lambda|h},1) = \frac{1}{h^2}\,[\,2\cos(|\lambda|h) + 2 - 4\cos(\frac{|\lambda|}{\sqrt{2}}h)\,]\,,$$

we are able to match $L_d(z_x,z_y)$ and $L(s_x,s_y)$ at 8 frequencies

$$(\,\omega_x\,,\,\omega_y\,) = (\,|\lambda|\cos(\frac{n}{4}\pi)\,,\,|\lambda|\sin(\frac{n}{4}\pi)\,)\,, \qquad 0 \le n \le 7\,.$$

as shown in Figure 1(c). Thus, (4.12) is the desired mode-dependent 9-point stencil discretization operator.

When $|\lambda|$ goes to zero, the Helmholtz equation reduces to the Laplace equation and schemes (4.10)-(4.12) converge to (4.5)-(4.7). So, schemes (4.10)-(4.12) can be viewed as a natural generalization of (4.5)-(4.7) and apply to both $\lambda=0$ and $\lambda\neq0$. The error estimate of the above schemes for the test functions $e^{s_xx+s_yy}$, where s_x and s_y satisfy the characteristic equation $s_x^2 + s_y^2 + \lambda^2 = 0$, can obtained straightforwardly. Since

$$\Delta(D_x,D_y)e^{s_xx+s_yy} = L_d(e^{D_xh},e^{D_yh})e^{s_xx+s_yy} = L_d(e^{s_xh},e^{s_yh})e^{s_xx+s_yy}\,,$$

we only have to replace E_x and E_y with e^{s_xh} and e^{s_yh} inside $L_d(E_x,E_y)$ and use a Taylor series expansion to simplify the resulting algebraic equation. By using this approach, we find that

$$L_{d,+}(e^{s_xh},e^{s_yh}) = (\,\frac{1}{24}\lambda^4 - \frac{1}{6}s_x^2s_y^2\,)\,h^2 + (\frac{-1}{480}\lambda^6 + \frac{1}{120}\lambda^2s_x^2s_y^2\,)\,h^4 + O(h^6)\,, \qquad (4.13)$$

$$L_{d,\times}(e^{s_xh},e^{s_yh}) = \frac{1}{3}s_x^2s_y^2h^2 - \frac{1}{30}\lambda^2s_x^2s_y^2h^4 + O(h^6)\,. \qquad (4.14)$$

Since $\gamma_+ = L_{h,+}(e^{i|\lambda|h},1)$ and $\gamma_\times = L_{h,\times}(e^{i\frac{|\lambda|}{\sqrt{2}}h}, e^{i\frac{|\lambda|}{\sqrt{2}}h})$, we also have

$$\gamma_+ = \frac{1}{24}\lambda^4 h^2 - \frac{1}{480}\lambda^6 h^4 + O(h^6)\,, \quad \gamma_\times = \frac{1}{12}\lambda^4 h^2 - \frac{1}{120}\lambda^6 h^2 + O(h^6)\,. \tag{4.15}$$

Combining (4.13)-(4.15), we have $\gamma_\times + \gamma_+ = O(h^2)$ and

$$(\gamma_\times+\gamma_+)L_{h,9}(e^{s_x h}, e^{s_y h}) = \gamma_\times L_{h,+}(e^{s_x h}, e^{s_y h}) + \gamma_+ L_{h,\times}(e^{s_x h}, e^{s_y h}) - \gamma_\times \gamma_+ = O(h^8)\,. \tag{4.16}$$

We know that both $L_{h,+}$ and $L_{h,\times}$ have an accuracy of $O(h^2)$ from (4.13) and (4.14), and that $L_{h,9}$ has an accuracy of $O(h^6)$ from (4.16). Note also that since the coefficients in front of h^2 in equations (4.13) and (4.14) are functions of λ, s_x and s_y for a fixed value of h, the above discretization schemes are less accurate when $|\lambda|$ is large.

Unlike in the ODE case, the mode-dependent schemes for PDEs cannot catch all modes in the null space of L, so that there exist discretization errors even for constant-coefficient PDEs. Rigorously speaking, the above error estimate applies only to constant-coefficient PDEs. If the coefficients of the PDE of interest are spatially varying, the error associated to mode-dependent schemes is still unknown. But, we suspect that when the coefficients are smoothly varying, the error is approximately the same as for constant coefficients.

Conventional finite-difference schemes for the Helmholtz equation are derived by discretizing the Laplacian with operators (4.5)-(4.7) and then combining them with the remaining term $\lambda^2 u$. The resulting schemes have all an accuracy of $O(h^2)$. Therefore, the conventional 9-point discretization scheme is much worse than the mode-dependent 9-point scheme. Although the conventional and mode-dependent 5-point schemes have the same order of accuracy, the mode-dependent schemes (4.10) and (4.11) are more accurate than conventional schemes along the contour (4.9). To show this, the discretization errors for mode-dependent and conventional 5-point discretization schemes are plotted in Figure 2 for the case where $\lambda = 10$ and $h = 0.1$.

On the other hand, we can also consider the discretization of the operator

$$\tilde{L}(D_x, D_y) = D_x^2 + D_y^2 - \lambda^2\,.$$

Considering only the real frequencies $(s_x, s_y) = (\sigma_x, \sigma_y)$, we have the characteristic equation,

$$\sigma_x^2 + \sigma_y^2 = \lambda^2 .$$

Thus, for the present case, we examine the σ_x–σ_y plane, instead of the ω_x–ω_y plane. By using an approach similar to the one described above, we get the following 5-point and 9-point stencil discretization schemes

$$\tilde{L}_{d,+}(E_x,E_y) = \frac{1}{h^2}\,[\,E_x^{-1} + E_x + E_y^{-1} + E_y - 4\cosh(\frac{|\lambda|}{\sqrt{2}}h)\,]\,,$$

$$\tilde{L}_{d,\times}(E_x,E_y) = \frac{1}{2h^2}\,[\,E_x^{-1}E_y^{-1} + E_x^{-1}E_y + E_xE_y^{-1} + E_xE_y - 4\cosh(|\lambda|h)\,]\,,$$

$$\tilde{L}_{d,9}(E_x,E_y) = \frac{\gamma_\times}{\gamma_\times+\gamma_+}\tilde{L}_{d,+}(E_x,E_y) + \frac{\gamma_+}{\gamma_\times+\gamma_+}\tilde{L}_{d,\times}(E_x,E_y) - \frac{\gamma_\times\,\gamma_+}{\gamma_\times+\gamma_+}\,,$$

where

$$\gamma_\times = \frac{1}{h^2}\,[\,\cosh(\sqrt{2}|\lambda|h) + 1 - 2\cosh(|\lambda|h)\,],\quad \gamma_+ = \frac{1}{h^2}\,[\,2\cosh(|\lambda|h) + 2 - 4\cosh(\frac{|\lambda|}{\sqrt{2}}h)\,]\,.$$

These schemes have an accuracy of $O(h^2)$, $O(h^2)$ and $O(h^6)$ respectively.

4.3 Convection-diffusion equation

For the convection-diffusion equation, the differential operator takes the form

$$L(D_x,D_y) = D_x^2 + D_y^2 - 2\alpha D_x - 2\beta D_y\,.$$

In particular, if we consider only real frequencies $(s_x,s_y) = (\sigma_x,\sigma_y)$, the corresponding characteristic equation is

$$\sigma_x^2 + \sigma_y^2 - 2\alpha\sigma_x - 2\beta\sigma_y = 0\,, \tag{4.17}$$

which is a circle in the σ_x-σ_y plane centered at (α , β) with radius $d = \sqrt{\alpha^2+\beta^2}$.

The conventional approach for discretizing the above equation relies on a central difference scheme to approximate the first and second order derivatives separately. This gives

$$L_{d,c}(E_x,E_y) = \frac{1}{h^2}\,[\,(1+\alpha h)E_x^{-1} + (1-\alpha h)E_x - 4 + (1+\beta h)E_y^{-1} + (1-\beta h)E_y\,]\,, \tag{4.18}$$

which corresponds to selecting a single coincident frequency at the origin. Allen and Southwell combined two 1D mode-dependent schemes along the x- and y-directions [1] (also see example 3 in Section 3). This leads to

$$L_{d,AS}(E_x,E_y)=\frac{1}{h}[\frac{2\alpha}{e^{2\alpha h}-1}(e^{2\alpha h}E_x^{-1}-1-e^{2\alpha h}+E_x)+\frac{2\beta}{e^{2\beta h}-1}(e^{2\beta h}E_y^{-1}-1-e^{2\beta h}+E_y)]. \tag{4.19}$$

which corresponds to selecting (0,0), (2α,0), (0,2β), (2α,2β) as coincident frequencies. Motivated by the discussion in the previous section, we select the coincident frequencies

$$(\sigma_x , \sigma_y) = (\alpha+d\cos(\frac{n}{2}\pi+\frac{1}{4}\pi) , \beta+d\sin(\frac{n}{2}\pi+\frac{1}{4}\pi)) , \qquad 0 \le n \le 3 ,$$

uniformly along the contour (4.17) and obtain the following stencil

$$L_{d,+}(E_x,E_y) = \frac{1}{h^2} [e^{\alpha h}E_x^{-1} + e^{-\alpha h}E_x + e^{\beta h}E_y^{-1} + e^{-\beta h}E_y - 4\cosh(\frac{d}{\sqrt{2}}h)] . \tag{4.20}$$

The multiplication of E_x by the factor $e^{-\alpha h}$ in the x-direction of the space domain corresponds to a shift in the s_x-coordinate in the transform domain, where s_x becomes $s_x - \alpha$, and a similar argument applies also to the y-direction. Therefore, the above scheme in fact shifts the center (α,β) of the circle (4.17) back to the origin and treats it as the Helmholtz equation with radius d. The coincident frequencies of these three schemes are plotted in Figure 3. Although all schemes have an accuracy of $O(h^2)$, schemes (4.19) and (4.20) are always diagonally dominant while the conventional scheme (4.18) loses this property for large cell Reynolds numbers αh and βh. This is one major disadvantage associated with the conventional central difference scheme.

Following a similar procedure, we can also design mode-dependent rotated 5-point and 9-point stencil discretization schemes for the convection-diffusion equation. This gives

$$L_{d,\times}(E_x,E_y) = \frac{1}{2h^2}[e^{(\alpha+\beta)h}E_x^{-1}E_y^{-1} + e^{(\alpha-\beta)h}E_x^{-1}E_y + e^{(-\alpha+\beta)h}E_xE_y^{-1} + e^{-(\alpha+\beta)h}E_xE_y - 4\cosh(dh)] , \tag{4.21}$$

$$L_{d,9}(E_x,E_y) = \frac{\gamma_\times}{\gamma_\times+\gamma_+}L_{d,+}(E_x,E_y) + \frac{\gamma_+}{\gamma_\times+\gamma_+}L_{d,\times}(E_x,E_y) - \frac{\gamma_\times\gamma_+}{\gamma_\times+\gamma_+} , \tag{4.22}$$

with

$$\gamma_\times = \frac{1}{h^2} [\cosh(\sqrt{2}dh) + 1 - 2\cosh(dh)], \quad \gamma_+ = \frac{1}{h^2} [2\cosh(dh) + 2 - 4\cosh(\frac{d}{\sqrt{2}}h)] .$$

These schemes have an accuracy of $O(h^2)$ and $O(h^6)$ respectively. Note that the constant $d = \sqrt{\alpha^2+\beta^2}$ in the convection-diffusion equation plays a similar role as the constant $|\lambda|$ in the Helmholtz equation. Therefore, as before, when $|\alpha|$ or $|\beta|$ becomes larger, the discretization

schemes (4.20)-(4.22) become less accurate for a fixed h.

5. Numerical Examples

We use the 1D and 2D convection-diffusion equations as test problems to demonstrate the efficiency of the mode-dependent finite-difference method.

(1) 1D test problem

Consider the 1D convection-diffusion equation on [0,1]

$$\frac{d^2u}{dx^2} - a(x)\,\frac{du}{dx} = 0\,, \quad \text{where} \quad a(x) = 10+\varepsilon\, x+\frac{\varepsilon}{10+\varepsilon\, x}\,, \tag{5.1}$$

with given $u(0)$ and $u(1)$. Our goal is to study the effect of the linear perturbation term $\varepsilon\, x$ on the accuracy of the mode dependent discretization scheme described in Section 3. Note that when $\varepsilon = 0$, the coefficient $a(x)$ is constant, and according to our analysis we expect that in this case the mode-dependent discretization will be exact. The term $\dfrac{\varepsilon}{10+\varepsilon\, x}$ is added so that (5.1) has the following analytic solution

$$u(x) = u(0) + [\,u(1) - u(0)\,]\,\frac{\exp(10x+0.5\varepsilon\, x^2)-1}{\exp(10+0.5\varepsilon) - 1}\,, \quad \text{where} \quad \exp(x) = e^x\,.$$

The boundary conditions $u(0) = 1$ and $u(1) = 10$ are selected. We compare the conventional and mode-dependent central difference schemes, i.e.

$$(1-\frac{a_n h}{2})U_{n+1} - 2U_n + (1+\frac{a_n h}{2})U_{n-1} = 0\,, \tag{5.2a}$$

$$\exp(-\frac{a_n h}{2})U_{n+1} - 2\cosh(\frac{a_n h}{2})U_n + \exp(\frac{a_n h}{2})U_{n-1} = 0\,, \tag{5.2b}$$

where $h = \dfrac{1}{N}$, $1 \le n \le N-1$, $U_0 = u(0)$ and $U_N = u(1)$.

First, we study the effect of the grid size h when the parameter $\varepsilon = 1$. Figure 4 shows that the errors of both schemes are proportional to $O(h^2)$. Furthermore, for this choice of ε and independently of the value of h, the error of the mode-dependent scheme is approximately 100 times smaller than for the conventional scheme. Next, we study the impact on the error of variations of the coefficient function $a(x)$. The first derivative of the coefficient function $a(x)$ is

approximately measured by the parameter ε, so that ε can be used as a measure of the local variations of $a(x)$. Errors versus ε for a fixed grid size $h = \frac{1}{16}$ are plotted in Figure 5. From this figure, we see that the conventional scheme is insensitive to changes in ε while the error of the mode-dependent scheme is proportional to $O(\varepsilon)$. Note that over the range of values of ε that we consider, the error of the mode-dependent scheme is considerably smaller than for the conventional scheme. However, by extrapolating the two error curves in Figure 5, it is clear that as ε becomes very large, i.e. as the coefficient function $a(x)$ deviates drastically from its nominal value $a = 10$, it will become preferable to use the conventional scheme. This suggests, as one would expect, that the mode-dependent discretization scheme should be employed only as long as we have a very approximate knowledge of the modes appearing in the solution.

(2) 2D test problems

We consider two 2D convection-diffusion equations on $[0,1]^2$ with Dirichlet boundary conditions associated with the given exact solutions, namely,

$$\textit{Example 1:}\quad \frac{\partial^2 u}{\partial x^2} + \frac{\partial^2 u}{\partial y^2} - \left(8+\varepsilon_x x+\frac{\varepsilon_x}{8+\varepsilon_x x} \right) \frac{\partial u}{\partial x} - \left(6+\varepsilon_y y+\frac{\varepsilon_y}{6+\varepsilon_y y} \right) \frac{\partial u}{\partial y} = 0, \quad (5.3)$$

with exact solutions

$$(1)\ \varepsilon_x = \varepsilon_y = 0, \quad u(x,y) = (0.2 + 6e^{8x})\ (0.01 + 2\, e^{6y}), \quad (5.4a)$$

$$(2)\ \varepsilon_x = \varepsilon_y = 0.002, \quad u(x,y) = [0.2 + 6\ \exp(8x+10^{-3}x^2)]\ [0.01 + 2\ \exp(6y+10^{-3}y^2)], \quad (5.4b)$$

and

$$\textit{Example 2:}\quad \frac{\partial^2 u}{\partial x^2} + \frac{\partial^2 u}{\partial y^2} - \left(8+\frac{2\varepsilon(\sigma_1-4)}{(1+\varepsilon x)\sigma_1+\varepsilon} \right) \frac{\partial u}{\partial x} - 6\,\frac{\partial u}{\partial y} = 0\,, \quad (5.5)$$

with exact solutions

$$(3)\ \varepsilon = 0, \quad u(x,y) = 10\exp[\ \sigma_1 x + \sigma_2\, y\ ]\,, \quad (5.6a)$$

$$(4)\ \varepsilon = 0.01, \quad u(x,y) = (1+10^{-2}x)\ 10\ \exp[\ \sigma_1 x + \sigma_2\, y\ ]\,, \quad (5.6b)$$

and where $\sigma_1 = 4+5\cos(\frac{15\pi}{16})$ and $\sigma_2 = 3+5\sin(\frac{15\pi}{16})$. We use the finite-difference schemes

(4.18)-(4.22) discussed in Section 4.3 to discretize (5.3) and (5.5) with grid size $h = \frac{1}{4}, \frac{1}{8}, \frac{1}{16}$ and $\frac{1}{32}$. The resulting systems of equations are solved by the SOR method for test cases (1) and (3) and by a local relaxation method described in [8], [26] and [27] for test cases (2) and (4). We plot the errors versus the grid size in Figures 6-9.

For test case (1), the solution contains four modes 1, e^{8x}, e^{6y} and e^{8x+6y}. In this case, since the Allen-Southwell scheme catches all these modes, it should be an exact method. Thus, the error plotted in Figure 6 represents the numerical rounding error instead of the discretization error. The other 5-point stencil discretizations give an error proportional to $O(h^2)$ for fine grids. The 9-point stencil scheme is considerably more accurate than the other 5-point stencil schemes. It comes close to the exact method when the grid size is $\frac{1}{32}$.

Test case (2) can be viewed as obtained from test case (1) by introducing linear perturbation terms $\varepsilon_x x$ and $\varepsilon_y y$ with $\varepsilon_x = \varepsilon_y = 0.002$ in the coefficient functions. We consider the effect of small variations of the coefficient functions. The Allen-Southwell scheme is not exact any longer, but still has a high accuracy. The 9-point discretization scheme has almost the same performance as the Allen-Southwell scheme. However, if we compare Figures 6 and 7, we see that the coefficient variations due to ε_x and ε_y make the error of the 9-point scheme 10 times as large as for the unperturbed case depicted in Figure 6. The accuracy of the other 5-point stencil schemes remains approximately the same.

For test case (3), the solution contains a single mode. All 5-point stencil discretization schemes have an accuracy of $O(h^2)$. The 9-point stencil discretization has an accuracy close to $O(h^6)$ for coarse grid sizes. Figure 8 shows also that although all 5-point stencil discretization schemes have a similar accuracy, the rotated 5-point operator $L_{d,x}(E_x, E_y)$ given by (4.21) is slightly more accurate than the Allen-Southwell scheme. As was noted earlier, this difference can be attributed to a different choice of coincident frequencies satisfying the characteristic equation (4.17)

Test case (4) is obtained by adding a perturbation term to test case (3). It appears that all 5-point stencil discretization schemes have a very similar accuracy in these two test cases. However, for the high-order 9-point stencil discretization, the perturbation makes the discretization error larger as the grid becomes finer. When $h = \frac{1}{32}$, the discretization error for the perturbed case (4) is approximately 10 times larger than for the unperturbed case (3).

From test cases (2) and (4), we may conclude that the mode-dependent discretization schemes still have a high accuracy for PDEs with nearly constant coefficients, but the 9-point stencil discretization is more sensitive to small variations of the coefficient functions than the 5-point stencil discretization schemes.

6. Related previous work

Although its properties were not always well understood, the mode-dependent finite-difference method has been discovered and rediscovered several times by a number of researchers and has been applied to the discretization of several types of ODEs and PDEs.

As was mentioned earlier, when the cell Reynolds number is large, the conventional central difference discretization of the convection-diffusion equation has convergence difficulties. Hence, the need for a mode-dependent scheme arises naturally when discretizing this equation, and more generally, when considering singular perturbation problems. Allen and Southwell [1] presented the first discretization of this type. A more detailed investigation of this scheme was performed by Dennis [12]. Since then, there have been a number of rediscoveries and elaborations such as [3] [9] [18] [28] [29] [35] [36] [39] [40]. Applications of Allen-Southwell's scheme to 2-D or 3-D fluid flow problems can be found in [2] [13]-[17] [37] [38] [41]. The methodology described in this paper can also be applied to the discretization of initial value ODEs. A mode-dependent finite-difference scheme for initial-value ODEs was first studied by Gautschi [19]. Some generalizations of Gautschi's work can be found in [5] [30] [34] [42] [43].

As shown in Sections 3 and 4, the transform domain approach is a convenient tool to derive mode-dependent discretization schemes on a uniform grid. However, the mode-dependent concept is so general that it also applies to nonuniform grids. Some researchers have used the mode-dependent idea to design finite-element methods, see e.g. [6] [10] [21]-[24] [33].

Interestingly, the mode-dependent scheme has been introduced under a number of different names such as the locally exact technique [3], the weighted-mean scheme [18], the smart upwind method [20], the optimal finite analytic method [32] and the upstream-weighted difference scheme [35].

7. Conclusions and Extensions

In this paper, we have used the spectral structure of differential operators to obtain more accurate finite-difference schemes. The transform domain point of view was shown to be simple and useful. For the case of homogeneous ODEs, we proposed a universal mode-dependent finite-difference scheme which is exact for constant-coefficient equations, and has a very high accuracy for equations with smoothly varying coefficients. For homogeneous PDEs, we considered mode-dependent 5-point, rotated 5-point and 9-point stencil discretizations of the Laplace, Helmholtz and convection-diffusion equations. The mode-dependent schemes for the Helmholtz and convection-diffusion equations turn out to be natural extensions of the schemes derived for the Laplace equation. We expect that the mode-dependent schemes that we have obtained will be quite useful for problems whose solution contains exponentially increasing or decreasing, or oscillatory components, provided that some very approximate information about these modes is available a priori. This information is usually revealed by the coefficients of the ordinary or partial differential equations of interest.

There exist similarities and differences between the mode-dependent finite-difference method and spectral methods. Both discretization techniques are based on a spectral analysis of the differential and difference operators and try to match their spectral properties. However, the spectral method analyzes spectra by using Fourier basis functions, i.e. functions with frequencies along the imaginary axis. In this approach, a large number of basis functions is usually required to synthesize a given function. Hence, in order to get a high degree of accuracy, more grid points are necessary and the resulting scheme is a global one. The mode-dependent finite-difference method enlarges the set of basis functions so that the spectral analysis can be performed in the entire transform domain. Since fewer basis functions are required to synthesize a function due to this enlargement, the resulting scheme is local. This local nature of the mode-dependent finite-difference method makes it easy to analyze and insensitive to boundary conditions. In contrast, spectral methods are relatively more complicated and sensitive to different types of boundary con-

ditions.

We basically focused on the discretization of a differential operator in the interior region and assumed the simplest Dirichlet boundary conditions throughout this paper. Since the finite-difference method is local, the discretization scheme for grid points in the interior region will not be affected by the specific nature of the boundary conditions. However, grid points along the boundary need some special treatment. Although the general mode-dependent concept should still apply in this case, some details need to be examined in later work. In addition, as mentioned above, it would be of interest to find a general procedure for estimating the error of mode-dependent finite-difference schemes when they are applied to varying-coefficient differential equations. Finally, it would also be interesting to study the application of the mode-dependent concept to the discretization of time-dependent partial differential equations.

Acknowledgement

The authors would like to thank Professor Lloyd N. Trefethen for his encouragements and helpful discussions.

References

1. D. N. De G. Allen and R. V. Southwell, "Relaxation Methods Applied to Determine the Motion, in Two Dimensions, of a Viscous Fluid Past a Fixed Cylinder," *Q. J. Mech. and Appl. Math.*, vol. 8, pp. 129-145, 1955.
2. D. N. De G. Allen, "A Suggested Approach to Finite-difference Representation of Differential Equations, with an Application to Determine Temperature-distributions near a Sliding Contact," *Q. J. Mech. and Appl. Math.*, vol. 15, pp. 11-33, 1962.
3. K. E. Barrett, "The Numerical Solution of Singular-Perturbation Boundary-Value Problems," *Q. J. Mech. and Appl. Math.*, vol. 27, pp. 57-68, 1974.
4. A. E. Berger, J. M. Solomon, M. Ciment, S. H. Leventhal, and B. C. Weinberg, "Generalized OCI Schemes for Boundary Layer Problems," *Math. Comp.*, vol. 35, no. 151, pp. 695-731, Jul. 1980.
5. D. G. Bettis, "Numerical Integration of Products of Fourier and Ordinary Polynomials," *Numer. Math.*, vol. 14, pp. 421-434, 1970.
6. W. S. Blackburn, "Letters to the Editor," *Int. J. Num. Meth. Eng.*, vol. 10, pp. 718-719, 1976.
7. R. F. Boisvert, "Families of High Order Accurate Discretizations of Some Elliptic Problems," *SIAM J. Sci. Stat. Comput.*, vol. 2, no. 3, pp. 268-284, Sep. 1981.
8. E. F. Botta and A. E. P. Veldman, "On Local Relaxation Methods and Their Application to Convection-Diffusion Equations," *Journal of Computational Physics*, vol. 48, pp. 127-149, 1981.
9. D. G. Briggs, "A Finite Difference Scheme for the Incompressible Advection-diffusion Equation," *Comp. Meth. Appl. Mech. Eng.*, vol. 6, pp. 233-241, 1975.
10. I. Christie, D. F. Griffiths, A. R. Mitchell, and O. C. Zienkiewicz, "Finite Element Methods for Second Order Differential Equations with Significant First Derivatives," *Int. J. Num. Meth. Eng.*, vol. 10, pp. 1389-1396, 1976.
11. G. Dahlquist, A. Bjorck, and N. Anderson, *Numerical Methods*, Prentice-Hall, Inc. , Englewood Cliffs, NJ. , 1974.
12. S. C. R. Dennis, "Finite Differences Associated with Second-Order Differential Equations," *Q. J. Mech. and Appl. Math.*, vol. 13, pp. 487-507, 1960.
13. S. C. R. Dennis, "The Numerical Solution of the Vorticity Transport Equation," in *Proc. of Third Int. Conf. Num. Meth. Fluid Mech.*, pp. 120-129, Springer-Verlag, New York, NY, 1973.
14. S. C. R. Dennis, D. B. Ingham, and R. N. Cook, "Finite-Difference Methods for Calculating Steady Incompressible Flows in Three Dimensions," *J. Comp. Phys.*, vol. 33, pp. 325-339, 1979.
15. S. C. R. Dennis, D. B. Ingham, and S. N. Singh, "The Steady Flow of a Viscous Fluid Due to a Rotating Sphere," *Q. J. Mech. Appl. Math.*, vol. 34, pp. 361-381, 1981.
16. S. C. R. Dennis, D. B. Ingham, and S. N. Singh, "The Slow Translation of a Sphere in a Rotating Viscous Fluid," *J. Fluid Mech.*, vol. 117, pp. 251-267, 1982.
17. T. M. El-Mistikawy and M. J. Werle, "Numerical Method for Boundary Layers with Blowing - The Exponential Box Scheme," *AIAA J.*, vol. 16, pp. 749-751, Jul. 1978.
18. M. E. Fiadeiro and G. Veronis, "On Weighted-mean Schemes for the Finite-difference Approximation to the Advection-diffusion Equation," *Tellus*, vol. 29, pp. 512-522, 1977.
19. W. Gautschi, "Numerical Integration of Ordinary Differential Equations Based on Trigonometric Polynomials," *Numer. Math.*, vol. 3, pp. 381-397, 1961.
20. P. M. Gresho and R. L. Lee, "Don't Suppress the Wiggles - They're Telling You Something," *Computers and Fluids*, vol. 9, pp. 223-253, 1981.
21. J. C. Heinrich, P. S. Huyakorn, O. C. Zienkiewicz, and A. R. Mitchell, "An 'Upwind' Finite Element Scheme for Two-Dimensional Convection Transport Equation," *Int. J. Num. Meth. Eng.*, vol. 11, pp. 131-143, 1977.

22. J. C. Heinrich and O. C. Zienkiewicz, "Quadratic Finite Element Schemes for Two-dimensional Convective-Transport Problems," *Int. J. Num. Meth. Eng.*, vol. 11, pp. 1831-1844, 1977.

23. P. S. Huyakorn, "Solution of Steady-state, Convective Transport Equation Using an Upwind Finite Element Scheme," *Appl. Math. Modelling*, vol. 1, pp. 187-195, Mar. 1977.

24. A. Kanarachos, "Boundary Layer Refinements in Convective Diffusion Problems," *Int. J. Num. Meth. Eng.*, vol. 18, pp. 167-180, 1982.

25. L. V. Kantorovich and V. I. Krylov, *Approximate Methods of Higher Analysis*, Interscinece Publishers, Inc., New York, 1964.

26. C.-C. J. Kuo, B. C. Levy, and B. R. Musicus, "A Local Relaxation Method for Solving Elliptic PDEs on Mesh-Connected Arrays," *SIAM J. Sci. Stat. Comp.*, vol. 8, no. 4, pp. 530-573, Jul. 1987.

27. C.-C. J. Kuo, B. C. Levy, "A Two-level Four-color SOR method," to apear in *SIAM Journal on Numerical Analysis*.

28. B. P. Leonard, "A Survey of Finite Differences with Upwinding for Numerical Modelling of the Imcompressible Convective Diffusion Equation," in *Computational Techniques in Transient and Turbulent Flow*, ed. C. Taylor & K. Morgan, Pineridge Press, Swansea, U.K., 1981.

29. W. Lick and T. Gaskins, "A Consistent and Accurate Procedure for Obtaining Difference Equations from Differential Equations," *Int. J. Num. Meth. Eng.*, vol. 20, pp. 1433-1441, 1984.

30. T. Lyche, "Chebyshevian Multistep Methods for Ordinary Differential Equations," *Numer. Math.*, vol. 19, pp. 65-75, 1972.

31. R. E. Lynch and J. R. Rice, "A High-Order Difference Method for Differential Equations," *Mathematics of Computation*, vol. 34, no. 150, pp. 333-372, Apr. 1980.

32. R. Manohar and J. W. Stephenson, "Optimal Finite Analytic Methods," *J. Heat Transfer*, vol. 104, pp. 432-437, Aug. 1982.

33. A. Moult, D. Burley, and H. Rawson, "The Numerical Solution of Two-Dimensional, Steady Flow Problems by the Finite Element Method," *Int. J. Num. Meth. Eng.*, vol. 14, pp. 11-35, 1979.

34. B. Neta and C. H. Ford, "Families of Methods for Ordinary Differential Equations Based on Trigonometric Polynomials," *Journal of Computational and Applied Mathematics*, vol. 10, pp. 33-38, 1984.

35. G. D. Raithby and K. E. Torrance, "Upstream-Weighted Differencing Schemes and Their Application to Elliptic Problems Involving Fluid Flow," *Computers and Fluids*, vol. 2, pp. 191-206, 1974.

36. D. F. Roscoe, "New Methods for the Derivation of Stable Difference Representations for Differential Equations," *J. Inst. Maths Applics*, vol. 16, pp. 291-301, 1975.

37. D. F. Roscoe, "The Solution of the Three-Dimensional Navier-Stokes Equations Using a New Finite Difference Approach," *Int. J. Num. Meth. Eng.*, vol. 10, pp. 1299-1308, 1976.

38. D. F. Roscoe, "The Numerical Solution of the Navier-Stokes Equations for a Three-Dimensional Laminar Flow in Curved Pipes Using Finite-Difference Methods," *J. Eng. Math.*, vol. 12, no. 4, pp. 303-323, Oct. 1978.

39. A. K. Runchal, "Convergence and Accuracy of Three Finite Difference Schemes for a Two-dimensional Conduction and Convection Problem," *Int. J. Num. Meth. Eng.*, vol. 4, pp. 541-550, 1972.

40. D. B. Spalding, "A Novel Finite Difference Formulation for Differential Expressions Involving Both First and Second Derivatives," *Int. J. Num. Meth. Eng.*, vol. 4, pp. 551-559, 1972.

41. N. C. Steele and K. E. Barrett, "A 2nd Order Numerical Method for Laminar Flow at Moderate to High Reynolds Numbers: Entrance Flow in a Duct," *Int. J. Num. Meth. Eng.*, vol. 12, pp. 405-414, 1978.

42. E. Stiefel and D. G. Bettis, "Stabilization of Cowell's Method," *Numer. Math.*, vol. 13, pp. 154-175, 1969.

43. P. J. Van Der Houwen and B. P. Sommeijer, "Linear Multistep Methods with Reduced Truncation Error for Periodic Initial-value Problems," *IMA Journal of Numerical Analysis*, vol. 4, pp. 479-489, 1984.

Figure Captions

Figure 1: Coincident frequencies of the mode-dependent (a) 5-point (b) rotated 5-point and (c) 9-point stencils discretizations of the Helmholtz equation.

Figure 2: Plot of $|\Delta(\omega_x,\omega_y)|$ as a function of c along the contour $(\omega_x,\omega_y) = (|\lambda|\cos(c\,\pi), |\lambda|\sin(c\,\pi))$, for (a) conventional and (b) mode-dependent 5-point stencil discretizations of the Helmholtz equation.

Figure 3: Coincident frequencies of the (a) central difference, (b) Allen-Southwell, and (c) uniformly-distributed mode-dependent 5-point stencil discretizations of the convection-diffusion equation.

Figure 4: l_∞-norm of the error versus the grid size h for (5.1) with $\varepsilon = 1$: (a) central difference scheme and (b) mode-dependent scheme.

Figure 5: l_∞-norm of the error versus the parameter ε for (5.1) with $h = \frac{1}{16}$: (a) central difference scheme and (b) mode-dependent scheme.

Figure 6: l_∞-norm of the error versus the grid size h for (5.4a) : (a) $L_{d,c}$, (b) $L_{d,AS}$, (c) $L_{d,+}$, (d) $L_{d,\times}$ and (e) $L_{d,9}$ given by (4.18)-(4.22).

Figure 7: l_∞-norm of the error versus the grid size h for (5.4b) : (a) $L_{d,c}$, (b) $L_{d,AS}$, (c) $L_{d,+}$, (d) $L_{d,\times}$ and (e) $L_{d,9}$ given by (4.18)-(4.22).

Figure 8: l_∞-norm of the error versus the grid size h for (5.6a) : (a) $L_{d,c}$, (b) $L_{d,AS}$, (c) $L_{d,+}$, (d) $L_{d,\times}$ and (e) $L_{d,9}$ given by (4.18)-(4.22).

Figure 9: l_∞-norm of the error versus the grid size h for (5.6b) : (a) $L_{d,c}$, (b) $L_{d,AS}$, (c) $L_{d,+}$, (d) $L_{d,\times}$ and (e) $L_{d,9}$ given by (4.18)-(4.22).

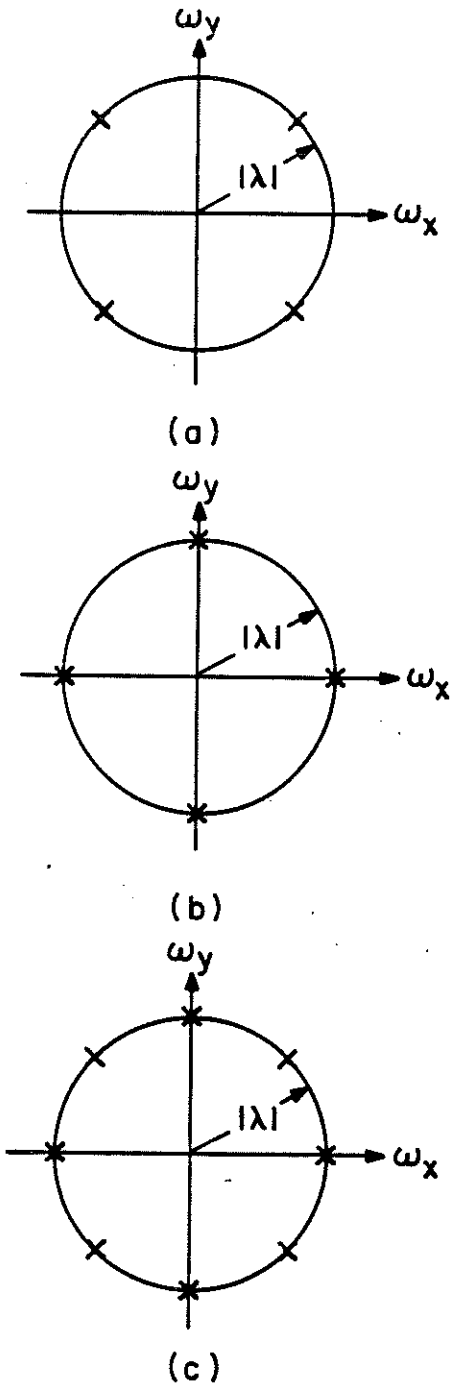

Figure 1: Coincident frequencies of the mode-dependent (a) 5-point (b) rotated 5-point and (c) 9-point stencils discretizations of the Helmholtz equation.

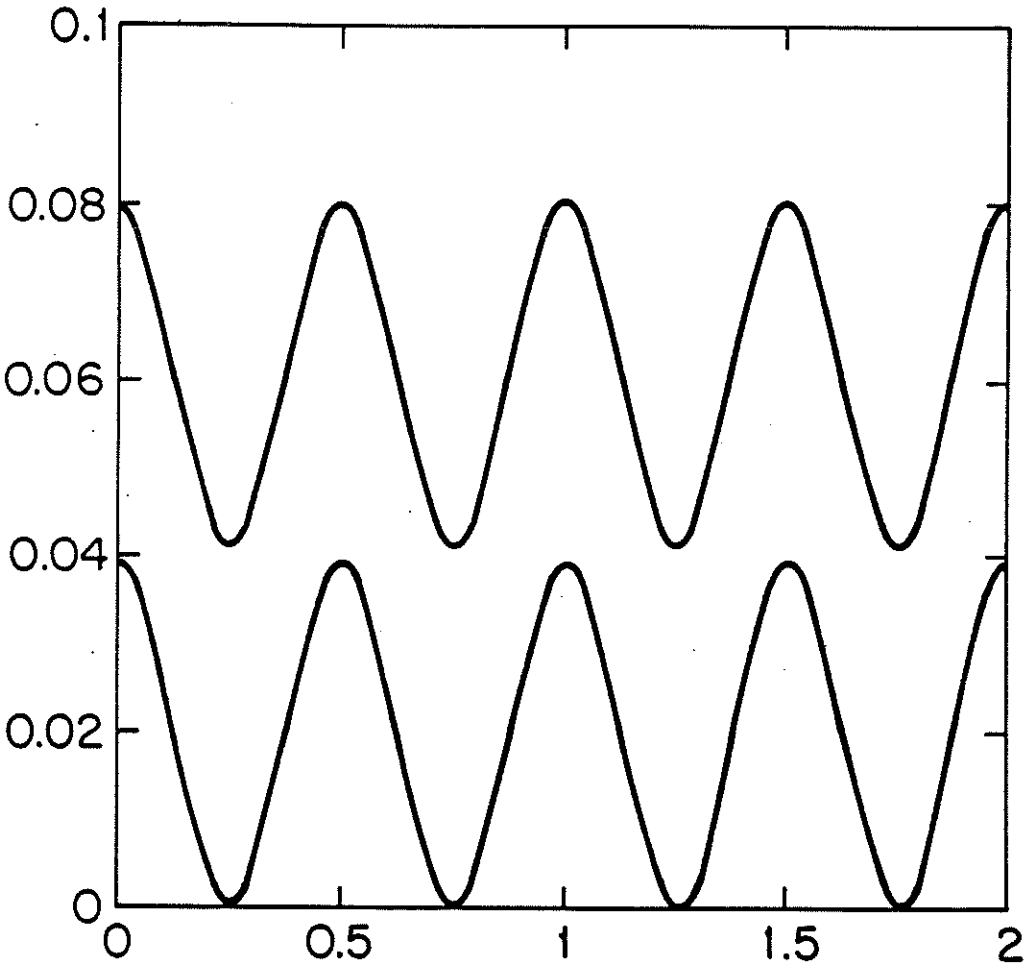

Figure 2: Plot of $|\Delta(\omega_x,\omega_y)|$ as a function of c along the contour $(\omega_x,\omega_y) = (|\lambda|\cos(c\,\pi), |\lambda|\sin(c\,\pi))$, for (a) conventional and (b) mode-dependent 5-point stencil discretizations of the Helmholtz equation.

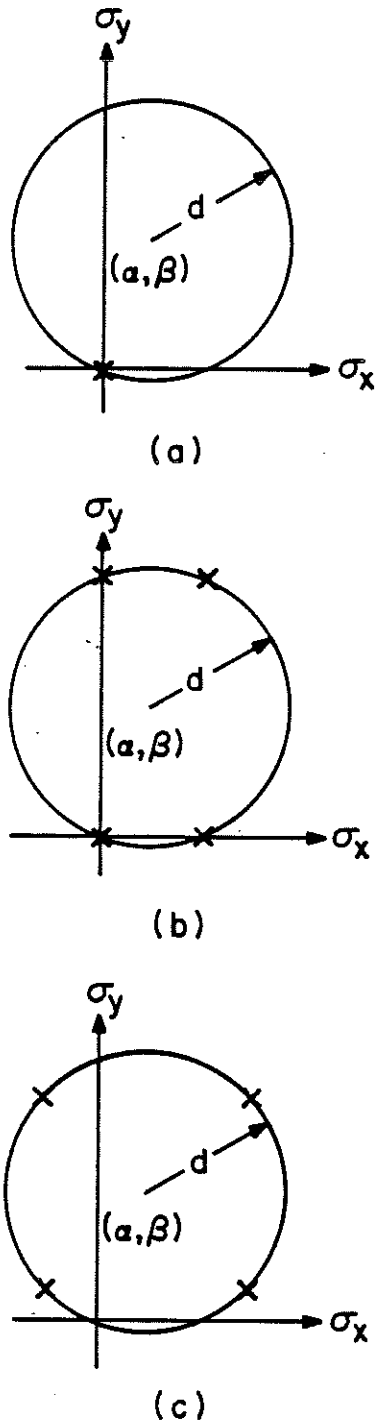

Figure 3: Coincident frequencies of the (a) central difference, (b) Allen-Southwell, and (c) uniformly-distributed mode-dependent 5-point stencil discretizations of the convection-diffusion equation.

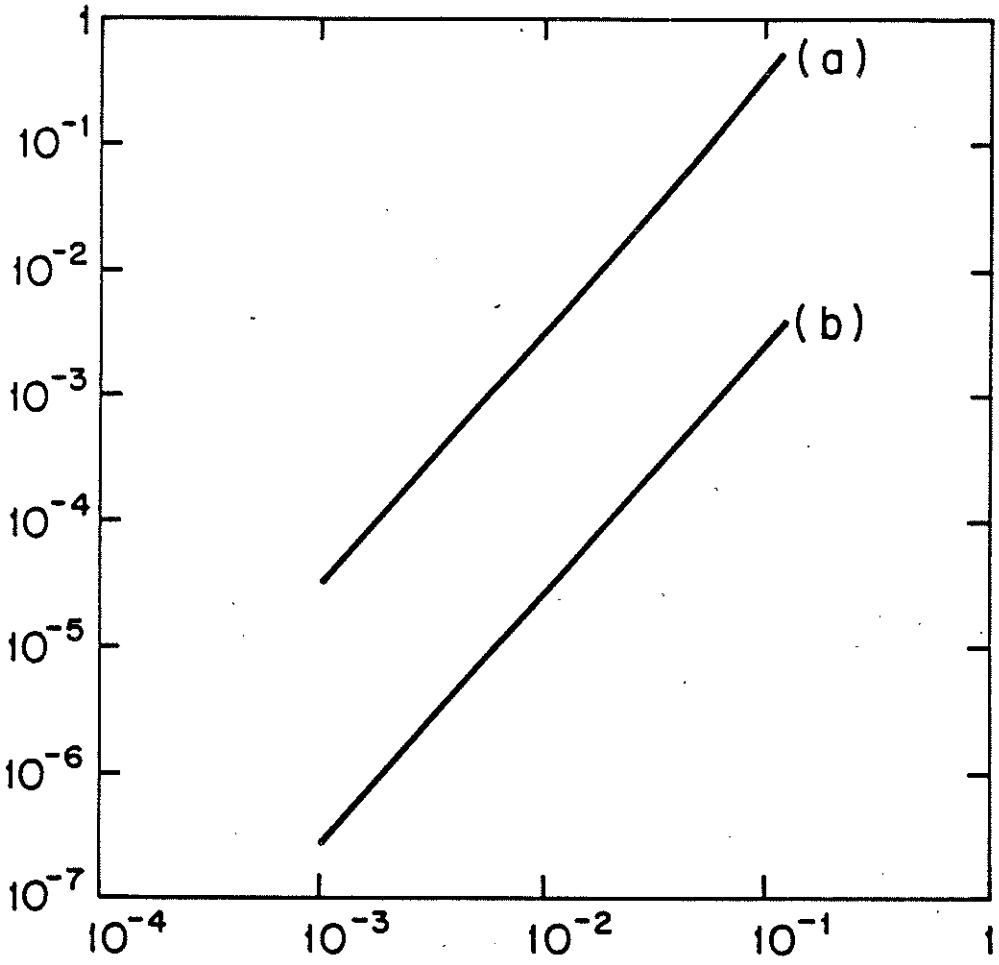

Figure 4: l_∞-norm of the error versus the grid size h for (5.1) with $\varepsilon = 1$: (a) central difference scheme and (b) mode-dependent scheme.

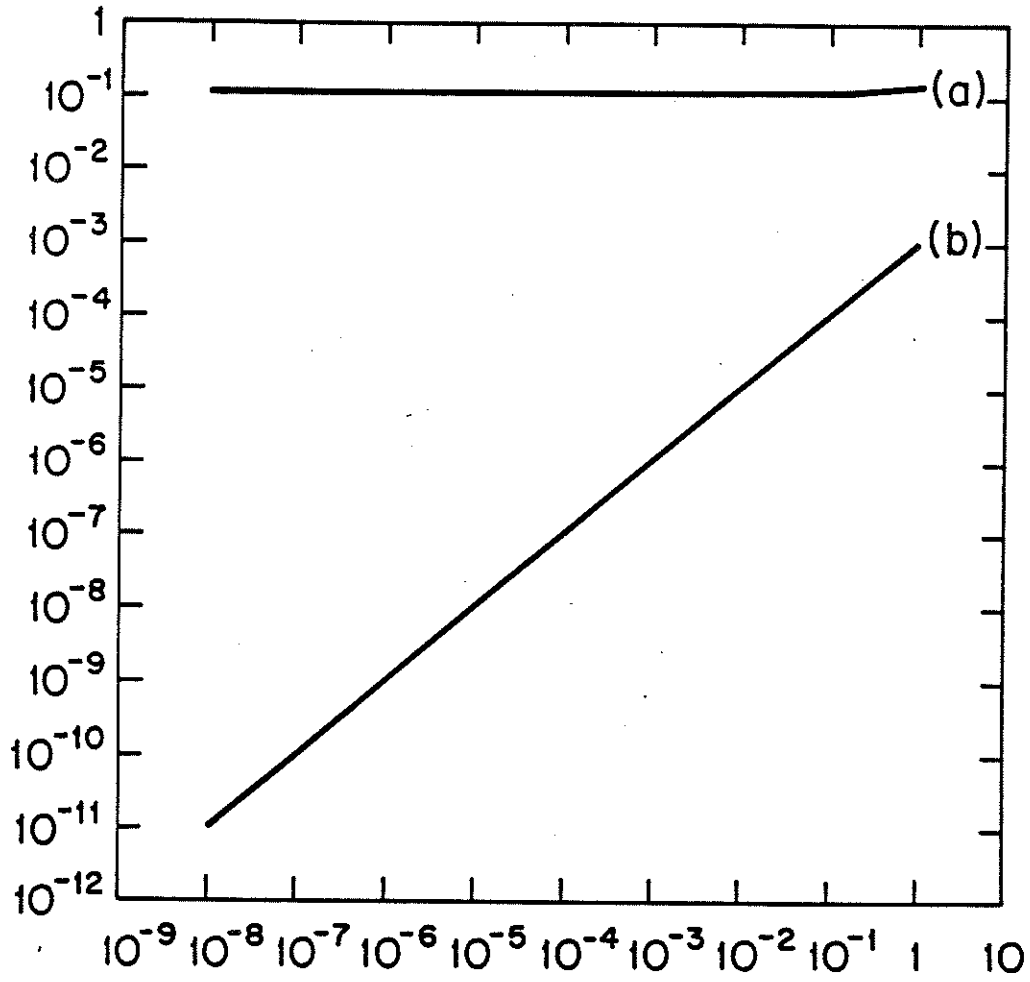

Figure 5: l_∞-norm of the error versus the parameter ε for (5.1) with $h = \frac{1}{16}$: (a) central difference scheme and (b) mode-dependent scheme.

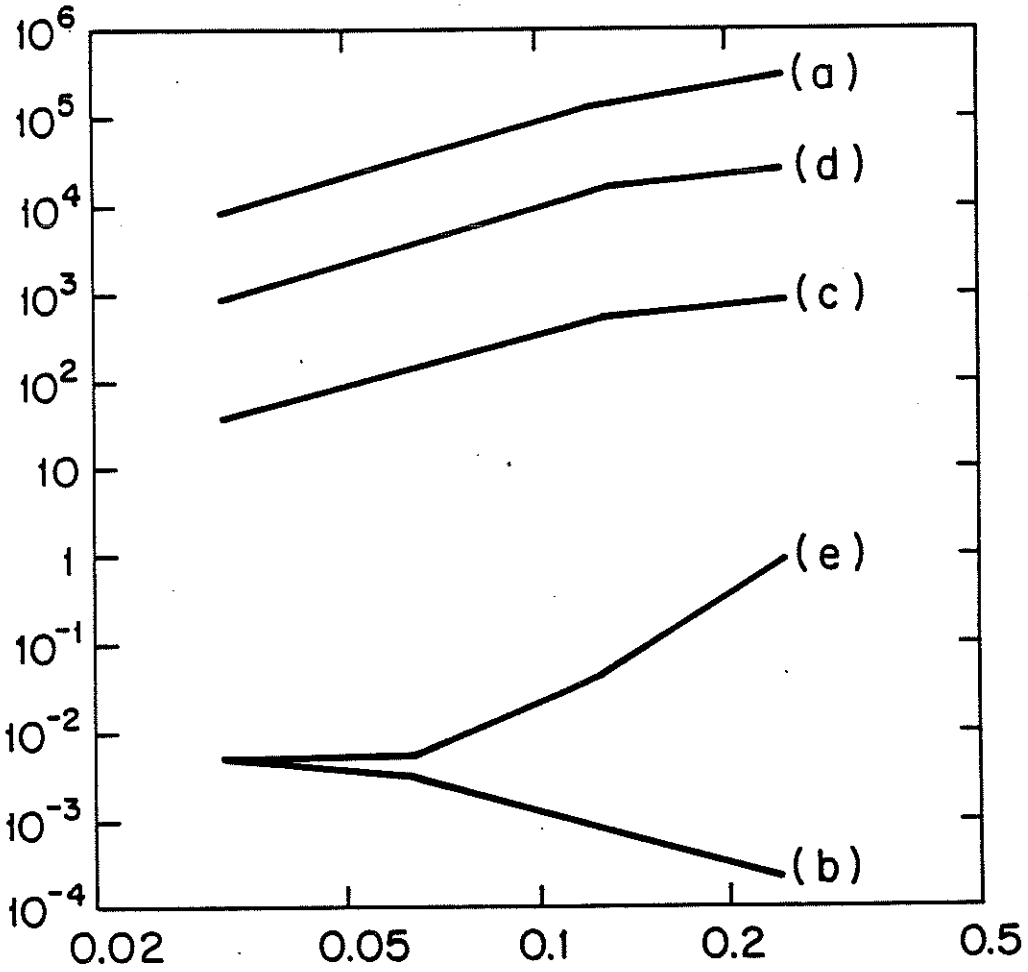

Figure 6: l_∞-norm of the error versus the grid size h for (5.4a) : (a) $L_{d,c}$, (b) $L_{d,AS}$, (c) $L_{d,+}$, (d) $L_{d,\times}$ and (e) $L_{d,9}$ given by (4.18)-(4.22).

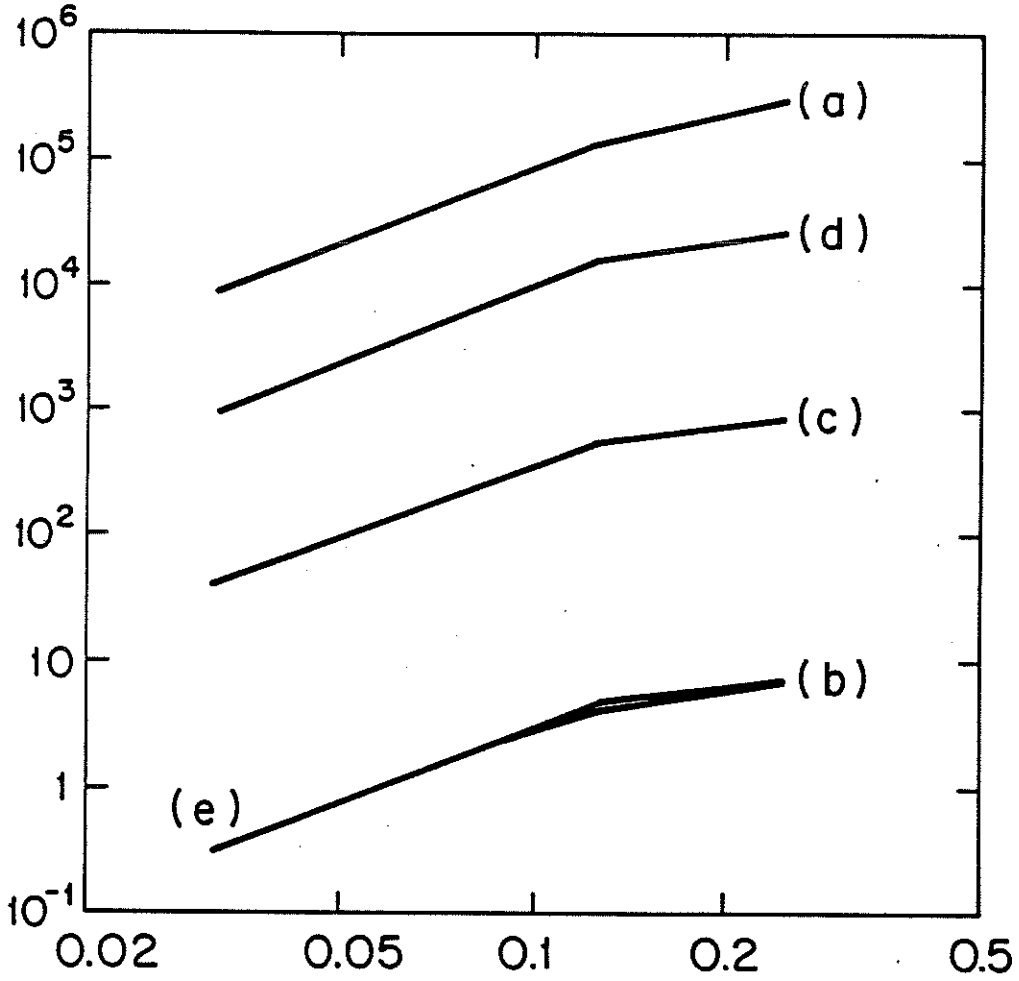

Figure 7: l_∞-norm of the error versus the grid size h for (5.4b) : (a) $L_{d,c}$, (b) $L_{d,AS}$, (c) $L_{d,+}$, (d) $L_{d,\times}$ and (e) $L_{d,9}$ given by (4.18)-(4.22).

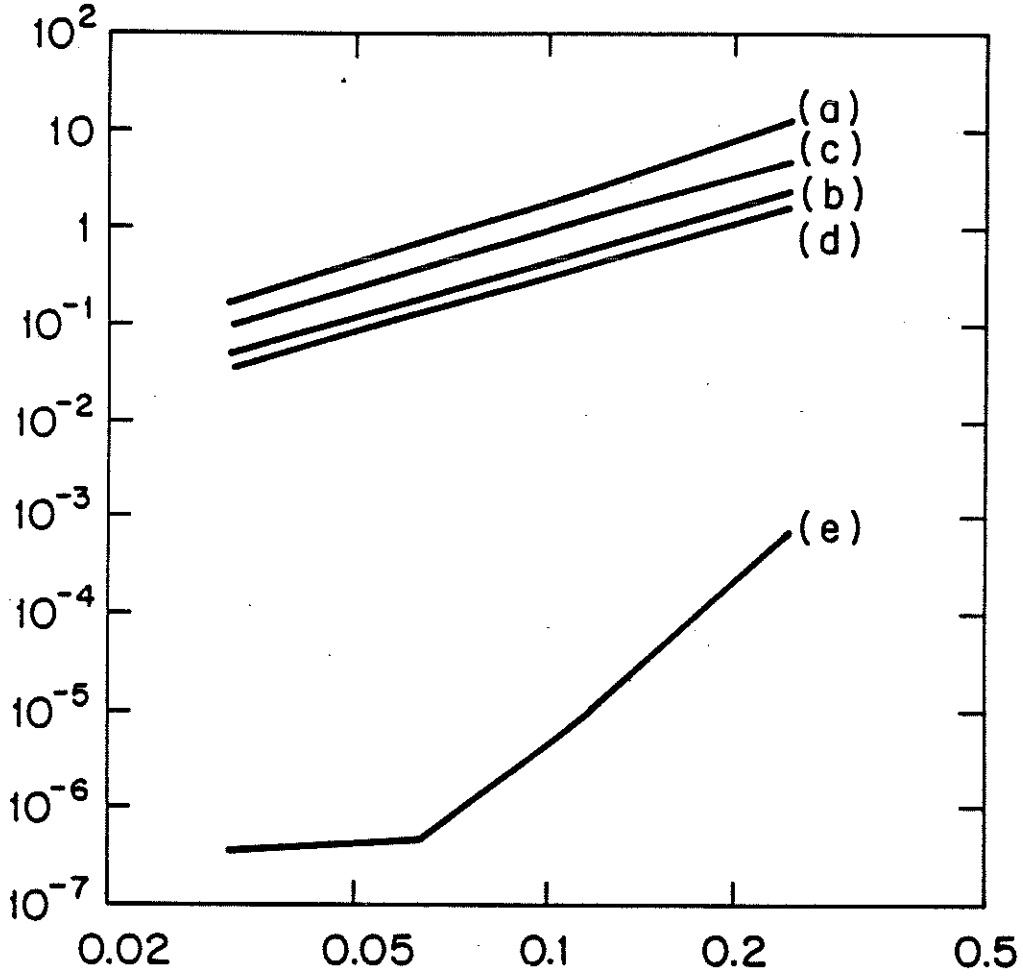

Figure 8: l_∞-norm of the error versus the grid size h for (5.6a) : (a) $L_{d,c}$, (b) $L_{d,AS}$, (c) $L_{d,+}$, (d) $L_{d,\times}$ and (e) $L_{d,9}$ given by (4.18)-(4.22).

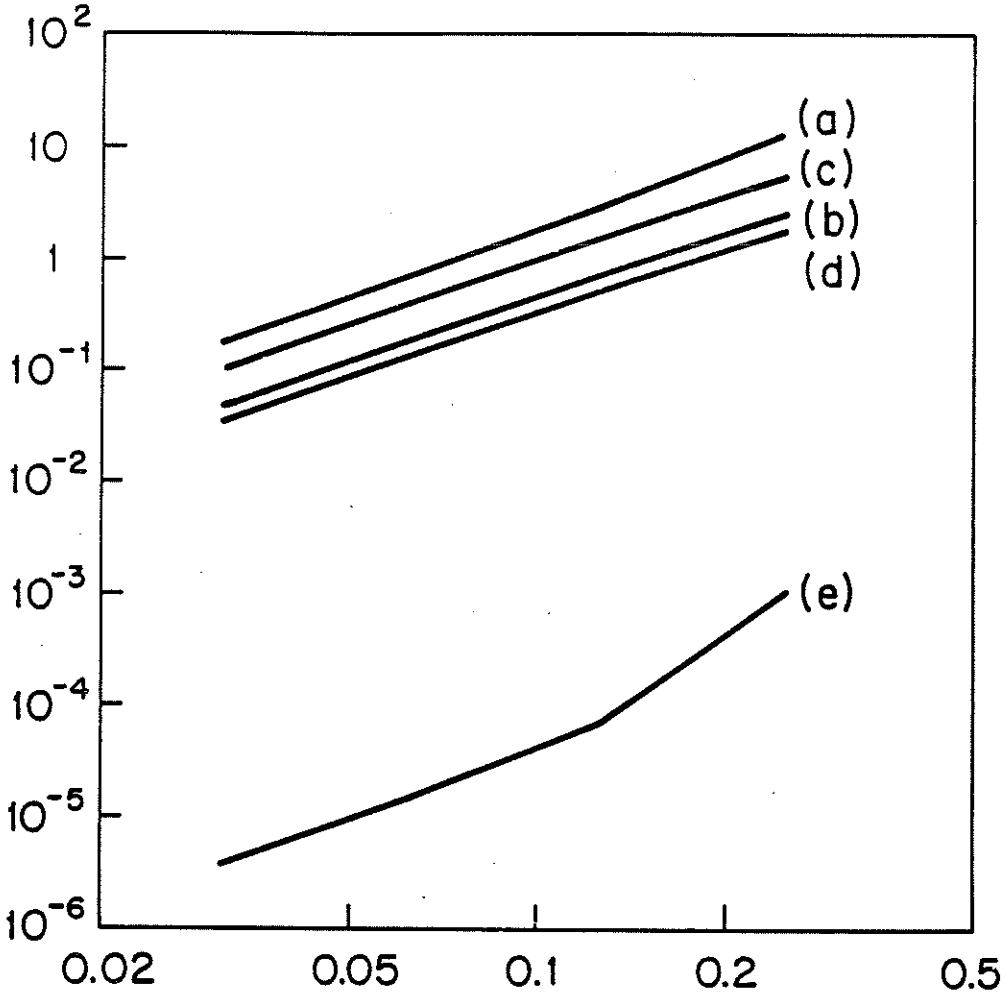

Figure 9: l_∞-norm of the error versus the grid size h for (5.6b) : (a) $L_{d,c}$, (b) $L_{d,AS}$, (c) $L_{d,+}$, (d) $L_{d,\times}$ and (e) $L_{d,9}$ given by (4.18)-(4.22).